

Shear-lag behavior of prestressed concrete box-girder bridges during balanced cantilever construction

Xingu Zhong^{*1}, Tianyu Zhang¹, Xiaojuan Shu¹ and Hongliang Xu²

¹School of Civil Engineering, Hunan University of Science and Technology; Hunan Provincial Key Laboratory of Structural Engineering for Wind Resistant and Vibration Control, Xiangtan, 411201, China

²China CEC Engineering, Corporation, Changsha, China

(Received December 21, 2016, Revised September 7, 2017, Accepted September 12, 2017)

Abstract. Balanced cantilever construction is extensively used in the construction of prestressed concrete (PSC) box-girder bridges. Shear-lag effect is usually considered in finished bridges, while the cumulative shear-lag effect in bridges during balanced cantilever construction is considered only rarely. In this paper, based on the balanced cantilever construction sequences of large-span PSC box-girder bridges, the difference method is employed to analyze the cumulative shear-lag effect of box girders with varying depth under the concrete segments' own weight. During cantilever construction, no negative shear-lag effect is generated, and the cumulative shear-lag effect under the balanced construction procedure is greater than the instantaneous shear-lag effect in which the full dead weight is applied to the entire cantilever. Three cross-sections of Jianjiang Bridge were chosen for the experimental observation of shear-lag effect, and the experimental results are in keeping with the theoretical results of cumulative shear-lag effect. The research indicates that only calculating the instantaneous shear-lag effect is not sufficiently safe for practical engineering purposes.

Keywords: box-girder bridges; balanced cantilever construction; shear-lag effect; the cumulative effect; prestress

1. Introduction

Due to the advantages of high stiffness, increased riding comfort, fewer expansion joints, low maintenance costs and wide span range, prestressed concrete constructed continuous (rigid-frame) box girder bridges have become a common design in freeway and urban road projects (Zhou *et al.* 2000). At present, most bridges of this kind are built using a cantilever construction technique. During construction, and with the cantilever gradually extending to its maximum length, the width-to-span ratio and depth-to-span ratio decrease while the self-weight increases. Recently, many theories and assumptions regarding the shear-lag effect of box girder bridges have been proposed (Cheng 1987, Guo 1983, Graham *et al.* 2010, Gara *et al.* 2009, Mondali *et al.* 2009), and some experimental investigations have also been conducted. These achievements solved many practical problems related to bridge structures, with some achieving widespread use in bridge

*Corresponding author, Professor, E-mail: 464397070@qq.com

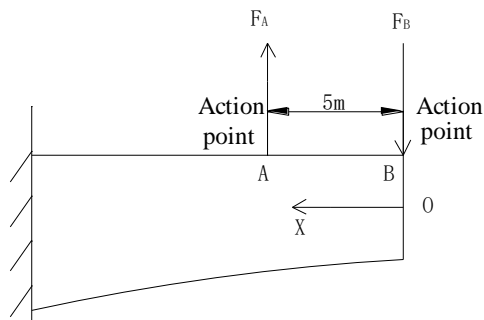


Fig. 1 Action points on cantilever by suspension

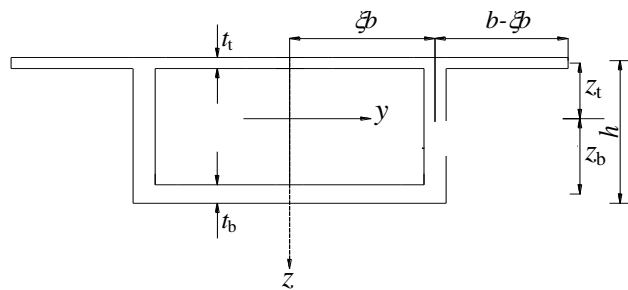


Fig. 2 Illustration of cross-section of box-girder

design specifications (National Standard of the People's Republic of China *et al.* 2004, AASHTO LRFD Bridge Design Specifications (SI Units) 3rd Edition 2004, Collection of German Standards for Bridge 1997). Most of the recent shear-lag theories (Luo 2005, Zhang and Wang 2004, Zhang *et al.* 1998) are built based on the mechanical behavior of finished bridges, while the cumulative effect of shear-lag induced by the variance of rigidity and self-weight during balanced cantilever construction of continuous (rigid-frame) box-girder bridges is not considered. Based on the study of Jianjiang Bridge, which is part of Xiarong Freeway (in Guizhou Province, China), this paper presents theoretical and experimental methods for evaluating the cumulative shear-lag effect in concrete box girder bridges during balanced cantilever construction. This research can also serve as a reference for the future studies on shear-lag effect in concrete box girder bridges with varying cross-sections.

2. Theoretical analysis of cumulative shear-lag effect

2.1 Governing equations

For simplification, box girder bridges are generally modeled as cantilevers (Luo 2005, Zhang and Wang 2004, Zhang *et al.* 1998) (shown in Fig. 1) subjected to either uniformly distributed loads or concentrated loads, and a typical cross-section of the box girder is shown in Fig. 2. It is taken that the plane section assumption suits the webs under symmetrical loads, and the transverse deformation as well as the out-of-plane shear deformation in webs are ignored.

Based on the principle of minimum potential energy, the first-order variation of the total

potential energy of the system will be zero, e.g.,

$$\delta\Pi = \delta(\bar{U} + \bar{V}) = 0 \quad (1)$$

where \bar{U} is the strain energy; and \bar{V} is the potential energy of the loading.

The potential energy of the loading is

$$\bar{V} = -\int_0^l q(x)w(x)dx \quad (2)$$

where $q(x)$ is the distributed load which is given by the weight per unit length of the bridge, l is the length of the bridge.

The strain energy \bar{U} is composed of the strain energy of the webs, the top slab and the bottom slab. The strain energy of the webs is

$$\bar{U}_w = \frac{1}{2} \int_0^l EI_w \frac{d^2w(x)}{dx^2} dx \quad (3)$$

where E is Young's modulus, and I_w is the moment of inertia of the webs.

The strain energy of the topslab is

$$\bar{U}_{st} = 2 \left\{ \frac{1}{2} \int_0^l \int_0^b t_t (E\varepsilon_{xt}^2 + G\gamma_t^2) dx dy \right\} \quad (4)$$

where

$$\varepsilon_{xt} = \frac{\partial u_t(x, y)}{\partial x}, \quad \gamma_t = \frac{\partial u_t(x, y)}{\partial y} \quad (5)$$

G is the shear modulus, t_t is the thickness of the top flange.

The potential energy of the bottom slab is

$$\bar{U}_{sb} = 2 \left\{ \frac{1}{2} \int_0^l \int_0^{\xi b} t_b (E\varepsilon_{xb}^2 + G\gamma_b^2) dx dy \right\} \quad (6)$$

where

$$\varepsilon_{xb} = \frac{\partial u_b(x, y)}{\partial x}, \quad \gamma_b = \frac{\partial u_b(x, y)}{\partial y} \quad (7)$$

t_b is the thickness of the bottom slab.

Thus, the total potential energy of the system in Eq. (1) is

$$\Pi = \bar{U}_w + \bar{U}_{st} + \bar{U}_{sb} + \bar{V} \quad (8)$$

Assuming that the longitudinal displacement of the flange can be described as a quartic parabolic distribution (Zhang *et al.* 1998), the longitudinal displacement of the top flanges $u_t(x, y)$ in Eq. (5) can be expressed as

$$u_t(x, y) = \begin{cases} Z_t \left[\frac{dw(x)}{dx} + \left(1 - \frac{y^4}{(\xi b)^4} \right) u(x) \right], & \text{if } |y| \leq \xi b \\ Z_t \left[\frac{dw(x)}{dx} + \left(1 - \frac{y^4}{(b - \xi b)^4} \right) u(x) \right], & \text{if } |y| > \xi b \end{cases} \quad (9)$$

and the longitudinal displacement of the bottom flanges $u_b(x, y)$ in Eq. (7) is expressed as

$$u_b(x, y) = Z_b \left[\frac{dw(x)}{dx} + \left(1 - \frac{y^4}{(\xi b)^4} \right) u(x) \right] \quad (10)$$

where $u(x)$ is maximum difference of angular rotation due to the shear deformation, $w(x)$ is the vertical displacement of the box girder, b is the half-width of the top slab, ξ is the reduction factor for the flange, Z_t and Z_b are the distance from the neutral axis to the center of the top slab and bottom slab, respectively.

The displacement $u(x)$ in Eqs. (9)-(10) is determined by the following differential equations and boundary conditions.

$$\frac{d^2 u(x)}{dx^2} - m \frac{du(x)}{dx} - k^2 u(x) = \frac{9n}{8E} Q(x) \quad (11)$$

$$\left[\frac{du(x)}{dx} - \frac{9}{8} n \frac{M(x)}{EI(x)} \right] \int_{x_1}^{x_2} \delta u(x) = 0 \quad (12)$$

where

$$m = \frac{9}{10} n \frac{d\alpha(x)}{dx}, \quad n = \frac{1}{1 - \frac{9}{10} \alpha(x)}, \quad \alpha(x) = \frac{I_s(x)}{I(x)}, \quad k^2 = \frac{45Gn}{14Eb^2}, \quad Q(x) = \frac{d}{dx} \left[\frac{M(x)}{I(x)} \right],$$

$Q(x)$ is the shearing force, $M(x)$ is the bending moment, $I_s(x)$ is the moment of inertia of the top and bottom slabs, $I(x)$ is the moment of inertia of the entire cross-section. It is noticed that the parameter m is close to zero and can be neglected in the equations.

The shear-lag moment is given by

$$M_F = \frac{4}{5} EI_s(x) \frac{du(x)}{dx} \quad (13)$$

Taking into account the shear-lag effect, the shear-lag coefficient is defined. The shear-lag coefficient at the intersection of the web and the flange is expressed by

$$\lambda_e = \frac{\sigma_e}{\sigma_o} = 1 + \frac{4}{5} \frac{I_s(x)}{I(x)} \left(\frac{EI(x)}{M(x)} \right) \frac{du(x)}{dx} \quad (14)$$

and the shear-lag coefficient at the center of the top slab is expressed by

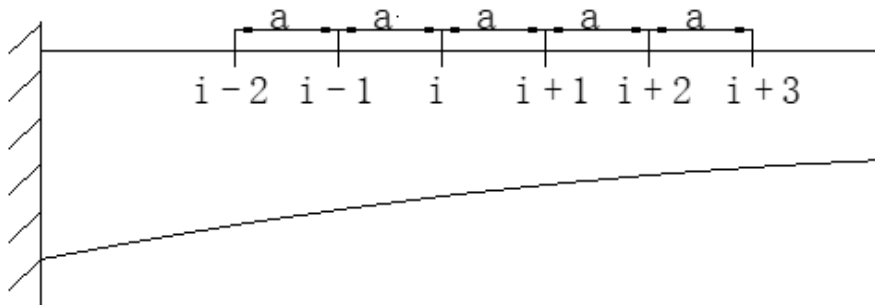


Fig. 3 Differential grid of cantilever with varying cross-section

$$\lambda_c = \frac{\sigma_c}{\sigma_o} = 1 - \left(1 - \frac{4 I_s(x)}{5 I(x)} \right) \left(\frac{EI(x)}{M(x)} \right) u(x) \tag{15}$$

where σ_o is the primary bending stress in cross-section, σ_e is the bending stress at the intersection of the web and flange, σ_c is the bending stress at the center of the top slab.

2.2 Employment of difference method

The general solution is unlikely to be solved from the above differential equations with variable coefficients. Thus, the difference method (Zhang and Wang 2004) is employed to obtain the approximate solutions.

Choosing an equidistant grid illustrated in Fig. 3, derivative in Eqs. (11)-(12) are replaced with the following difference quotient

$$\left. \begin{aligned} \left(\frac{du(x)}{dx} \right)_i &= \frac{u_{i+1} - u_{i-1}}{2a} \\ \left(\frac{d^2u(x)}{dx^2} \right)_i &= \frac{u_{i+1} - 2u_i + u_{i-1}}{a^2} \end{aligned} \right\} \tag{16}$$

in which a is the step size.

Substituting Eq. (16) into Eq. (11), one can obtain the following equation

$$u_{i-1} - (2 + a^2 k_i^2) u_i + u_{i+1} = \frac{9 a^2 n_i}{4 E} Q_i \tag{17}$$

The boundary conditions of Eq. (12) can be written as follows

$$\left[\frac{u_{i+1} - u_{i-1}}{2a} - \frac{9}{8} \frac{n_i}{EI_i} \right] \int_{x_1}^{x_2} \delta u = 0 \tag{18}$$

The shear-lag moment in Eq. (13) and shear-lag coefficients in Eqs. (14)-(15) are, respectively, written as follows

Table 1 Self-weight of cantilever segments (Unit: kN)

No.	Weight								
1	2896.7	6	2744.8	11	2480.9	16	1672.6	21	1472.1
2	2792.7	7	2630.4	12	2369.6	17	1617.5	22	1458.3
3	2691.8	8	2520.7	13	2266.2	18	1569.4		
4	2594	9	2416.2	14	2081	19	1528.8		
5	2499.4	10	2599.5	15	1823.9	20	1496.3		

Table 2 Geometric sizes of each cross-section (Unit: m)

Location coordinate	Bottom slab thickness	Web thickness	Section height	Location coordinate	Bottom slab thickness	Web thickness	Section height
0	0.350	0.5	4.500	48	0.636	0.8	6.905
4	0.352	0.5	4.531	52	0.685	0.8	7.266
8	0.358	0.5	4.605	56	0.739	0.8	7.649
12	0.368	0.5	4.713	60	0.797	0.8	8.054
16	0.382	0.5	4.852	64	0.858	0.8	8.478
20	0.400	0.5	5.020	68	0.924	0.8	8.924
24	0.421	0.5	5.215	72	0.993	0.8	9.389
28	0.447	0.5	5.436	76	1.067	0.8	9.874
32	0.477	0.5	5.683	80	1.144	0.8	10.379
36	0.511	0.5	5.954	84	1.225	0.8	10.903
40	0.548	0.7	6.248	88	1.311	0.8	11.446
44	0.590	0.8	6.565	92	1.400	0.8	12.008

$$M_F = \frac{4}{5} EI_{si} \frac{u_{i+1} - u_{i-1}}{2a} \quad (19)$$

$$\lambda_e = \frac{\sigma_e}{\sigma_0} = 1 + \frac{4}{5} \frac{I_{si}}{I_i} \left(\frac{EI_i}{M} \right) \frac{u_{i+1} - u_{i-1}}{2a} \quad (20)$$

$$\lambda_c = \frac{\sigma_c}{\sigma_0} = 1 - \left(1 - \frac{4}{5} \frac{I_{si}}{I_i} \right) \left(\frac{EI_i}{M} \right) \frac{u_{i+1} - u_{i-1}}{2a} \quad (21)$$

3. Application of theoretical method

3.1 Description of Jianjiang bridge

To apply the model, the shear-lag effect of Jianjiang Bridge will be analyzed using the above method. The main part of Jianjiang Bridge is a three-span prestressed concrete constructed continuous (rigid-frame) box girder bridge with a main span of 200 m and two side spans of 105 m. The main girder is single-box-single-cell box girder, and its depth is a parabola of order 1.75

(with 12 m-depth at the root and 4.5 m-depth at the mid-span). The top slab of the girder is 13 m wide and 0.3 m deep. The bottom slab is 7 m wide, and its depth is a quadratic parabola (0.35 m deep at the root and 1.4 m deep at the mid-span). Along the bridge span, the width of the webs is either 0.5 m or 0.8 m. At the pier, the top and bottom slabs are, respectively, 0.5 m and 1.5 m deep, and the webs are 1.0 m wide. The bridge is constructed using the balanced cantilever technique with rhombic travelling formworks. Each cantilever consists of 22 segments (except for the segment above the pier), in which 5 segments are 3.5 m long, 4 segments are 4 m long and 13 segments are 4.5 m long. The cantilever of each rhombic travelling formwork is 5.5 m long, and the two action points (shown in Fig. 1) of the rhombic travelling formwork are 5 m away from each other. The self-weight of the 22 segments are listed in Table 1, and the geometric sizes of each cross-section are listed in Table 2.

3.2 Calculation of cumulative shear-lag effect for Jianjiang bridge

The shear lag of representative stage structures upon phase instantaneous load is analyzed. Those were selected according to structural stiffness, load characteristics and theoretical analysis results. These include construction stages of No. 6, No. 10, No. 16, No. 22 beam cantilever construction stages, in which the structural length are respectively close to 1/4, 2/5, 3/4, 1 length of the whole cantilever.

Taken as an example of the shear-lag effect of balanced cantilever construction, the shear-lag effect was analyzed when the construction of Jianjiang Bridge reached segment No. 6. The length of the cantilever between segment No. 0 and No. 6 is 22 m. Giving the step size of 2 m, 11 integral grids were divided, and 11 linear equations were obtained from Eqs. (17)-(18), e.g.,

$$[K]\{u\} = \{Q\} \tag{22}$$

where

$$[K] = \begin{bmatrix} -(4+2a^2k_0^2) & 4 & 0 & \dots & 0 \\ 2 & -(4+2a^2k_1^2) & 2 & 0 & \dots \\ 0 & 2 & -(4+2a^2k_2^2) & 2 & 0 \dots \\ \vdots & \vdots & \vdots & \vdots & \vdots \\ 0 & 0 & \dots & 2 & -(4+2a^2k_{10}^2) \end{bmatrix},$$

$$\{u\} = \{u_0, u_1, u_2, \dots, u_{10}\}^T$$

$$\{Q\} = \frac{9a^2}{4E} \{n_0Q_0, n_1Q_1, n_2Q_2, \dots, n_{10}Q_{10}\}^T \text{ is the load matrix.}$$

Denoting the weight of the newly cast concrete segment as G , the reactions at the two acting points of the segment can be derived as $F_A=0.55G$ and $F_B=1.55G$, and the bending moment is given by the following expression

$$M = \begin{cases} F_B x, & \text{if } x \leq 5 \\ F_B x - F_A (x - 5) & \text{if } x > 5 \end{cases} \tag{23}$$

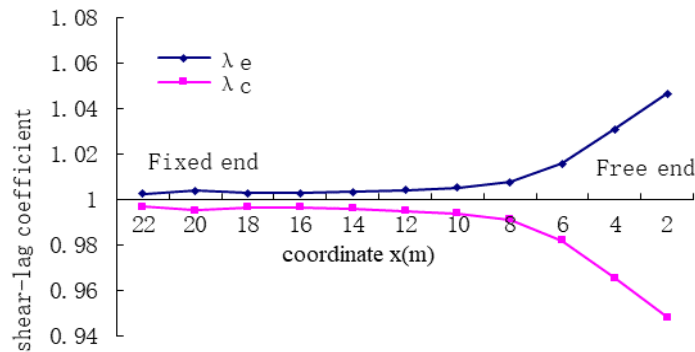


Fig. 4 Shear-lag coefficient λ_e induced by the action of newly constructed segment No.7

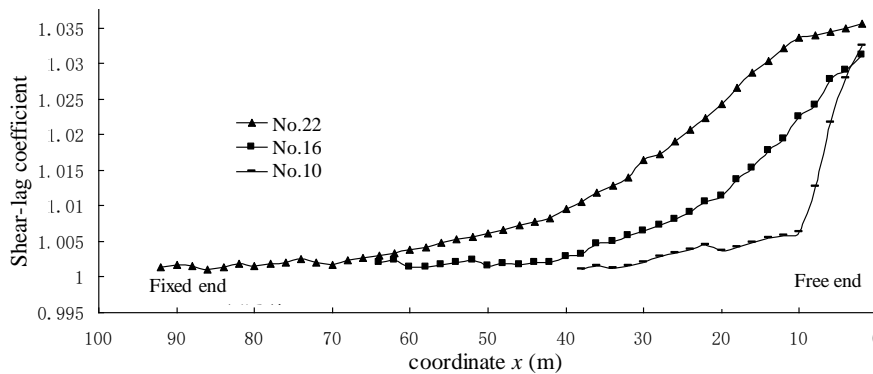


Fig. 5 Shear-lag coefficient λ_e induced by the action of newly constructed segments No.10, No.16 and No.22

Thus, the internal force Q_i at each integral point can be calculated by

$$Q_i = \frac{1}{n_i} \left[\frac{M_{i+1}}{I_{i+1}} - \frac{M_i}{I_i} \right] \tag{24}$$

The shear-lag coefficients can be calculated from Eqs. (19)-(21). The theoretical analysis of the shear lag is calculated by the fortran program written by the author. Fig. 4 illustrates the shear-lag coefficients of the previously constructed six segments induced by the weight of the newly constructed segment No. 7. The calculation shows that there is a positive shear lag effect in the cantilever subjected to the weight of concrete segments.

Using similar calculations, the shear-lag coefficients of the cantilever induced by the weight of segments No. 10, No. 16, and No. 22 were also calculated (shown in Fig. 5), respectively. From Fig. 5, it is shown that the shear-lag coefficient of the same segment increases with the ongoing cantilever construction.

In this paper, the effect of instantaneous shear lag is the effect of the finished structure under the phase load. Because the stage construction load-the weight of current constructing segment and the hanging basket was acting on partial segment of the finished structure, the structure produces a positive shear lag effect. And the cumulative shear lag effect obtained by superposition of each stage effect must be positive, so the shear lag effect of the whole cantilever considering construction is positive.

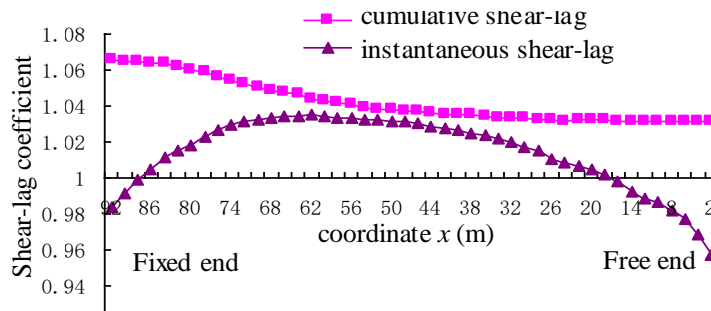


Fig. 6 Comparison of cumulative and instantaneous shear-lag coefficients λ_e

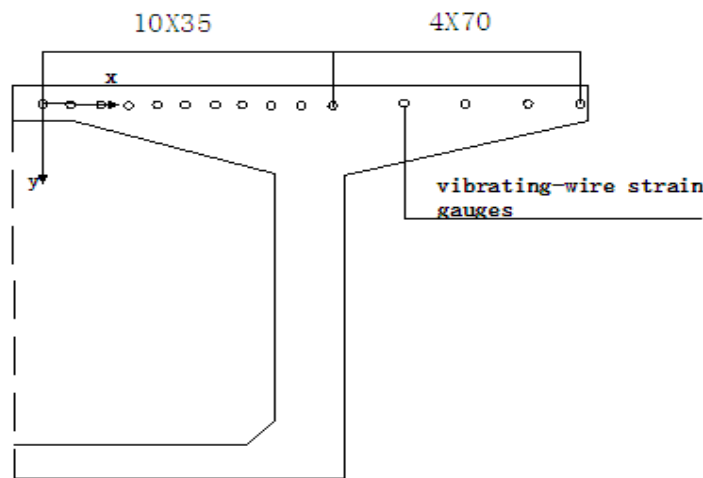


Fig. 7 Layout of strain sensor

3.3 Comparison between the cumulative and instantaneous shear-lag coefficients

The cumulative shear-lag coefficient λ_e at any cross-section after the cantilever construction was completed can be obtained by accumulating the corresponding shear-lag effect induced by the self-weight of each segment during the balanced cantilever construction. The calculated cumulative shear-lag coefficient λ_e of Jianjiang Bridge is illustrated in Fig. 6. It can be seen that the cumulative shear-lag coefficient at any cross-section is positive. Ignoring the balanced cantilever construction of the bridge, the instantaneous shear-lag coefficient which is based on the mechanical behavior of the finished bridge is also calculated and illustrated in Fig. 6. From the curve of instantaneous shear-lag coefficient in Fig. 6, it can be seen that a negative value exists at the free end.

From Fig. 6, the comparison between the cumulative and instantaneous shear-lag coefficient indicates that the cumulative shear-lag coefficient is always larger than the instantaneous shear-lag coefficients, and a large error exists at the free end and fixed end in the calculation of instantaneous shear-lag coefficient. It can be seen that these results agree well with the investigation of other researchers (Zhang *et al.* 1998). Since the cumulative shear lag effect is the superposition effect of different construction stages, while the shear lag effect of a cantilever structure is calculated according to the definite stiffness of the maximum cantilever structure

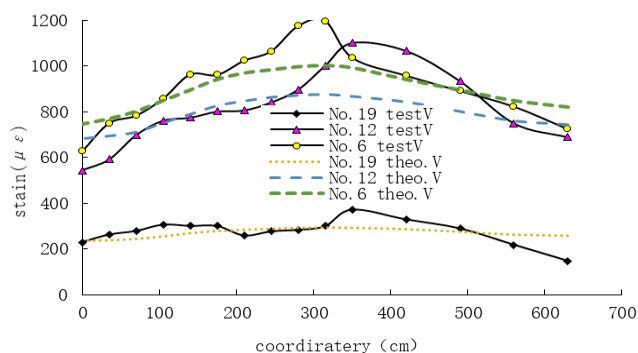


Fig. 8 Distribution of strain in measured cross-sections

loaded by the self-weight, so they result into big difference. In addition, since the shear lag effect is affected by the boundary condition, the error caused by the difference in the calculation of the shear lag effect at the ends is also increased.

4. Test of shear-lag effect of Jianjiang bridge during cantilever construction

In the construction process of the left half of Jianjiang Bridge, the end sections of segments No.6 (cantilever length of 22 m), No. 12 (cantilever length of 39.5 m) and No. 19 (cantilever length of 78.5 m) of the cantilever at the sixth pier were instrumented for measuring the cumulative shear-lag effect. The strain sensors were embedded in the top slab of the three cross-sections, and all sensors were fixed on the underside of the top reinforcement. The axis of the sensors was parallel to the longitudinal axis of the bridge and the center of the sensors was 10 cm away from the top surface of the bridge. The sensors were all vibrating-wire strain sensors, and their layout is shown in Fig. 7. All sensors were spaced at 70 cm in the cantilever flange and 35 cm in the top flange.

The readings of the sensors before and after concrete casting were recorded and their differences were equal to the self-weight of the newly cast concrete segment. The cumulative values of the strains in the three cross-sections are shown in Fig. 8. The abscissa in Fig. 8 corresponds to the x-axis in Fig. 7). From Fig. 8, it is shown that the largest strain in the cross-section is located at the intersection of the webs and flange, while the strains at the outer edge of the top flange ($x=0$) and the center of the top slab ($x=630$) are relatively small. According to the definition of cumulative shear-lag coefficient in Eq. (11), the shear lag coefficient at the location near the fixed end will be much larger than any location farther away from the fixed end, which agrees well with the calculated result of the cumulative shear-lag coefficient. Furthermore, all test data of strain in the three cross-sections indicates that the shear-lag effect is always positive, which also agrees well with the theoretical result.

5. Conclusions

- The theoretical result of the cumulative shear-lag coefficient considering balanced cantilever construction of box-girder bridges indicates that the shear-lag effect is always positive, while the

instantaneous shear-lag coefficient without considering balanced cantilever construction provides a negative value at the free end. The largest cumulative shear-lag coefficient is located at the fixed end, while the instantaneous shear-lag coefficient at the fixed end has a small value. The calculated results of the theoretical method considering the balanced cantilever construction agrees well with the test results of Jianjiang Bridge. The accordance of the theoretical and test results shows the proposed theoretical method used to analyze the shear-lag effect of box-girder bridges is valid.

- The calculated cumulative shear-lag coefficient is always larger than the instantaneous shear-lag coefficient, which implies the instantaneous shear-lag coefficient underestimates the shear-lag effect of the bridge. Thus, the traditional bridge design based on the calculation method of instantaneous shear-lag coefficient is not safe enough. It is necessary to consider the balanced cantilever construction procedure in practical bridge construction when studying the shear-lag effect of bridges. The research in this paper may supply an improved calculation method of shear-lag effect for the current bridge design theory.

Acknowledgments

This work is partially supported by the National Natural Science Foundation of China (No.51678253).

References

- AASHTO LRFD Bridge Design Specifications (SI Units), (2004), *American Association of State Highway and Transportation Officials*, 3rd Edition, Washington, U.S.A.
- Cheng, Q.Y. (1987), "The negative shear-lag in thin-walled cantilever box girder", *Chin. Quarter. Mech.*, **2**, 52-62.
- Collection of German Standards for Bridge (1997), *Highway Planning and Design Institution of the Department of Transportation*.
- Gara, F., Leoni, G. and Dezi, L.A. (2009), "A beam finite element including shear lag effect for the time-dependent analysis of steel-concrete composite decks", *Eng. Struct.*, **31**(8), 1888-1902.
- Graham, D.A., Carradine, D.M. and Bender, D.A. (2010), "Monotonic and reverse-cyclic loading of lag screw connections for log shear wall construction", *J. Mater. Civil Eng.*, **22**(1), 88-95.
- Guo, J.Q., Fang, Z.Z. and Luo X.D. (1983), "Analysis of shear-lag effect of box girder bridges", *Chin. J. Civil Eng.*, **16**, 1-13.
- Luo, Q.Z. (2005), "Theoretical and experimental study on shear-lag in thin-walled box girder based on energy principle", Ph.D. Dissertation, Hunan University, Changsha, China.
- Mondali, M., Abedian, A. and Ghavami, A. (2009), "A new analytical shear-lag based model for prediction of the steady state creep deformations of some short fiber composites", *Mater. Des.*, **30**(4), 1075-1084.
- National Standard of the People's Republic of China (2004), *Code for Design of Highway Reinforced Concrete and Prestressed Concrete Bridges and Culverts*, China Communications Press, Beijing, China.
- Zhang, S.D. and Wang, W.Z. (2004), *The Negative Shear-Lag Effect of Bridge Structures*, 1st Edition, China Communications Press, Beijing, China.
- Zhang, S.D., Deng X.H. and Wang, W.Z. (1998), *The Shear-Lag Effect of Thin-Walled Box Girder*, 1st Edition, China Communications Press, Beijing, China.
- Zhou, J.S. and Lou, Z.H. (2000), "The status quo and developing trends of large span prestressed concrete bridges with continuous rigid frame structure", *J. Chin. High.*, **13**(1), 31-36.